Nano-electrochemical deposition of fuel cells electrocatalysts

MK MATHE [a,*], TS MKWIZU [a,b], I CUKROWSKI [b]
[*,a]CSIR Materials Science and Manufacturing, Energy and Processes, PO Box 395, Pretoria, 0001
[b]Department of Chemistry, University of Pretoria, Pretoria, 0002
Email: kmathe@csir.co.za

Abstract

This paper reports on the development of automated electrochemical deposition method as a synthetic strategy for fabrication of catalytically-active thin-films (or nanostructured) materials, composed of Platinum Group Metals (PGMs), with potential technological applications in fuel cell electrodes. The paper demonstrates the versatility of part-by-part (sequential) electrodeposition of binary alloys composed of Platinum and Ruthenium, to produce catalytic-active layers on an inert carbon substrate, whereby such fabricated bimetallic systems exhibit superior activity towards oxidation of methanol, a typical fuel used in Direct Methanol Fuel Cell, as compared to the pure platinum catalysts.

1. Introduction

Among the most crucial components in fuel cells are the electrodes (anodes and cathodes) at which electrochemical reactions (reactions which liberate or consume electrons from breakdown of molecules) take place. The flow of such electrons is one of the fundamental aspects in generating electricity from fuel cells. For these reactions to occur at useful rates either the operating temperature has to be high or electrocatalysts have to be used, a scenario particularly crucial at low operating temperatures desired for mobile applications of fuel cells and their miniaturized versions – micro-fuel cells – for typical applications such as powering of laptops by fuel cells in place of conventional batteries.

Electrocatalysis concerns rates of interfacial chemical reactions taking place between electrodes (solid surfaces) and molecules in solution or gas phase. Properties of electrodes (e.g. Catalytic/Electrocatalytic Activity) depend on controlled variation of the particle sizes, shapes, and dispersion of constituent elements of the given electrode surface.

It is known in catalysis research that the size of particles influences the activity, not only due to the enhanced surface area, but also due to particular electronic properties different from those of bulk materials. Confinement of electrons in small metal particles considerably changes the electronic band structure and therefore the chemical bonding behaviour of reacting molecules on the catalytic particles. Consequently, tailoring the size and shape of metal or semiconductor structures allows for tuning the electronic and catalytic properties according to desired applications. There is a strong drive to implement strictly surface modifications of electrode materials by combination of nanostructured multi-metallic elements for use as electrocatalysts in an elegant, well-controlled way. However, synthesis of nanostructured binary, ternary, or multi-element catalysts, with maximised atomic contact (and thus catalyst utilisation) of the constituent particles, still remains a challenge.

Bimetallic or even multi-metallic and alloy catalyst formulations have been a particularly vigorous area of research with regards to low-temperature fuel cells (Watanabe, 2003, Mathiyarasu et al., 2004, Koper, 2004). Multi-metallic catalysts used to improve the carbon monoxide (CO) tolerance of the hydrogen oxidation or to enhance alcohol oxidation activity in fuel cell anodes have been reported (Vigier et al., 2006, Goddard et al., 2006, Antolini, 2007), whereas on the cathode side it has recently been established that for oxygen reduction certain bimetallic surfaces have superior activity compared to pure platinum (Toda et al., 1999, Watanabe, 2003). Enhancement of catalytic activity of multi-metallic surfaces in comparison to pure metal surfaces is now attributed to ligand (or electronic) and bifunctional effects (Roth et al., 2008). Bifunctional effects involve the combination of distinctive catalytic properties of each of the elements in the alloy, in a synergistic fashion, resulting in a catalytic surface that is more active than each of the elements alone. In ligand or electronic effects one of the elements alters the electronic properties of the other so as to yield a more active catalytic surface. Literature studies suggested that the ratio of Platinum (Pt) to Ruthenium (Ru) has a dramatic effect on the performance of the Pt-Ru catalyst for oxidation of alcohols in Direct Alcohol Fuel Cells (DAFCs) (Chu and Gilman, 1996, Iwasita et al., 1994, Yajima et al., 2004). The issue of optimal composition and size effects is still an ongoing challenge (Petrii, 2008). Therefore, catalyst fabrication techniques that can be convenient for controlling the catalyst loading and atomic ratio composition of the multi-metallic catalysts would be useful.

Various methods are being used to fabricate electrocatalysts including thermal decomposition of precursors (chemical sources of desired catalytic materials), vacuum-based chemical vapour deposition techniques, chemical deposition using reducing agents, and electrochemical deposition, among others. Controlling the primary structures of the constituent elements in multi-element materials require control of the growth with respect to size, shape, crystal structures and composition of the underlying particles because these primary structures determine the physical and chemical properties of materials produced (Watanabe, 2003). The main challenge in all cases is to have good dispersion and control of particle sizes as well as maximizing proximity of the catalytic particles to active areas of electrode surfaces and increase utilization of, particularly, the expensive noble metallic catalysts such as platinum.

Electrochemical deposition on solid surfaces is a relatively low-cost, simple, and efficient method to prepare metal nanoparticles dispersed on solid surfaces. Electrochemical deposition presents the advantage that the driving force for metal formation from appropriate precursors (the substrate potential) can be controlled more precisely and on a much shorter time scale than in alternative processes - for example, chemical reduction - allowing the required control of the growth process. Electrodeposition of binary or ternary alloys by conventional methods are typically performed with either a preformed layer containing one metal or codeposition of metals of interest from a common electrolytic bath. The main problem with nanoparticle electrodeposition by codeposition is that the only control points are the deposition potential, or current density, in most cases. Also, codeposition has frequently resulted in deposits with poor crystallinity and side-products. It is not always the case that such conditions are optimal for the depositing elements in cases of binary and ternary alloys (Stickney et al., 2002).

Sequential electrodeposition techniques such as Electrochemical Atomic Layer Deposition (EC-ALD) (Gregory and Stickney, 1991, Stickney et al., 2002, Mathe et al., 2004, Kim et al., 2006, Venkatasamy et al., 2006) are increasingly being demonstrated to be robust alternative electrochemical synthetic methods offering more control over the growth of nano-scaled structures for potential applications in nano-optical, nanomagnetic, nano-electronic or energy devices.

EC-ALD was identified as a potential catalyst fabrication technique. EC-ALD (also referred to as EC-ALE; ALE for Atomic Layer Epitaxy) is an electrochemical deposition method that involves alternated electrodeposition of atomic layers of elements on a substrate, employing underpotential deposition (UPD) in which one element deposits onto another element at a voltage prior to that necessary to deposit the element onto itself (Stickney et al., 2002). These deposition processes are typically carried out at ambient temperatures and use small concentrations of precursor solutions (typically in millimolar levels). Different solutions are used to deposit each element separately. EC-ALD is an attractive technique because of the inherent advantages of sequential electrochemical deposition with self-limiting growth of deposits, features that may allow, for instance, fine-tuning of catalytic properties in relation to ratios of constituent elements, by way of stopping the growth of deposits at appropriate points. So far the focus of investigations of improving electrodeposition methods by using EC-ALD/EC-ALE mechanisms, for controlled growth of thin-film deposits, has been performed for deposition of thin-film compounds or alloys involving elements in the periodic table groups II to VI (Stickney et al., 2002, Mathe et al., 2004). As far as relevance to electrocatalysis is concerned, formation of Pt nanofilm on single-crystalline gold substrate via EC-ALD methodology has been demonstrated recently (Kim et al., 2006).

Controlled film growth of binary or ternary alloys or inter-metallic nano-materials involving noble metals fabricated via the EC-ALD routes has not been explored extensively.

This work aims to demonstrate the versatility of automated sequential electrodeposition in syntheses of nanostructured electrocatalysts via a process referred to as surface-limited redox-replacement reactions (SLR^3) involving spontaneous replacement of copper (Cu) templating layers in synthesis of multilayers composed of noble metals Pt and/or Ru as monometallic or bimetallic systems. The basis of our work is to expand on very recent developments in formation of platinum or ruthenium as monometallic nanostructures/nanofilms supported on single-crystal oriented gold substrate as demonstrated in the literature in an automated EC-ALD (Kim et al., 2006, Thambidurai et al., 2008). In this work we explore an extension to SLR^3 synthetic strategies towards formation of bimetallic systems, whereby each constituent metal is deposited via an SLR^3 deposition cycle. The methodology explored here involves formation of alternate multilayers (Pt-Ru) sequentially deposited via replacement of sacrificial Cu layers for controlling the deposition of each noble metal. We also demonstrate the inherent advantages of sequential electrodeposition using flow-cells as opposed to batch cells in probing electrocatalytic activities of the as-prepared electrocatalysts using the same electrochemical flow-cells used in their preparation; the approach that we deem to be useful in stepwise synthesis of multi-metallic catalysts with respect to tuning of their catalytic properties. Glassy carbon (GC) was used as a model carbonaceous substrate, keeping in mind that carbon materials are still the ubiquitous catalyst supports in fuel cell applications. A few reports have appeared recently in which manual electrodeposition of Pt or Au monometallic structures in batch electrochemical cells were grown on GC via redox-replacement of Cu or Pb templating layers (Tegou et al., 2007, Papadimitriou et al., 2007). Our work expands on these reports by using a fully-automated procedure in electrochemical flow-cells as opposed to batch cells.

2. Development of an automated electrochemical deposition setup

Another advantage of sequential electrochemical deposition is that the process can be automated. A number of automated instrumental setups have been described in the literature (Colletti et al., 1998, Huang et al., 1995, Villegas and Napolitano, 1999, Pezzatini et al., 1999, Innocenti et al., 2001, Flowers Jr. et al., 2002, Zhu et al., 2005). The hardware components required for a typical sequential electrodeposition automated setup can be generalised as follows:

- Solutions reservoirs (Precursor elements and rinse solutions)
- Solutions distribution system (Pumps and Valves)
- Source of inert gas (Oxygen exclusion mechanism)
- Electrochemical (Deposition) Cell
- Potentiostat
- Computer with necessary data acquisition system

The time required to complete each step in the deposition cycle is generally accomplished by (i) the intrinsic parameters of the deposition process (such as kinetics); and (ii) parameters associated with the cell geometry and solution delivery. Villegas (Villegas and Napolitano, 1999) suggested the following design criteria in relation to EC-ALD and the quality of deposits:

- Potential control must be maintained at all times during the deposition process.
- Solutions must be delivered to the deposition cell in a continuous fashion while allowing the precursors to remain in contact with the electrode just long enough for each deposition step to be completed.
- The precursors must be rinsed out of the cell completely and efficiently before the next deposition step to avoid co-deposition of the two elements.
- The cell and the solution-delivery manifold must be made entirely of materials that can be cleaned effectively to ensure purity of the deposits.

In this work, we have adopted virtual instrumentation principles to develop a general-purpose laboratory–scale automated instrumentation for electrochemical deposition of nanomaterials sequentially. Virtual instrumentation can simply be defined as combining hardware and software with industry-standard computer technologies to create user-defined instrumentation solutions. In virtual instruments the same set of stand-alone hardware components can perform different tasks imposed on them by the software (Walters, 1995).

The apparatus used in this work consisted of various commercially-available hardware components as well as (i) four model 765 Dosimats (Metrohm, Switzerland) configured as piston pumps with Teflon pistons, connected to Pyrex bottles; (ii) a 5-way rotatable multi-valve positioner (model R36781 valve head and model R77810 valve drive, Hamilton, Switzerland), (iii) a thin-layer electrochemical flow-through cell with three electrodes, (iv) potentiostat (Autolab PGSTAT 30 – Metrohm, Switzerland), and (v) personal computer. Polytetrafluoroethylene (PTFE) tubing and fittings (nuts and ferrules) were used for delivery of reagents from pyrex stock bottles to the electrochemical flow-cell. A schematic diagram of the experimental setup and a custom-built flow-cell are presented in Figure 1. In the instrumental setup, the pumps are controlled via a personal computer using the RS-232 interface. Pump parameters that can be controlled are the flow rate and volume of solution to dispense. The pumps can also be operated manually, which gives some flexibility in using them as multi-purpose pumps. The rotary 5-way valve (4 inlets and 1 outlet) consists of a fixed stator and a movable rotor. The stator is connected to the valve body in a manner that allows attachment of tubing, sample loops and other devices. The movable rotor is simply positioned to connect one of the inlet lines to the outlet channel. Up to four different solutions can be independently delivered to the flow-cell via the outlet channel of the rotary valve. The potentiostat is computer-controlled via a Universal Serial Bus (USB) interface. Computer programs for operation of the setup have been developed in-house using LabVIEW.

The thin-layer electrochemical cell was a custom-built flow-cell described in Figure 1(B) with a flow-channel defined by a 1 mm-thick silicone rubber gasket which was cut to expose an oval opening, 0.6 cm wide and 1.5 cm long, which held approximately 120 µL.

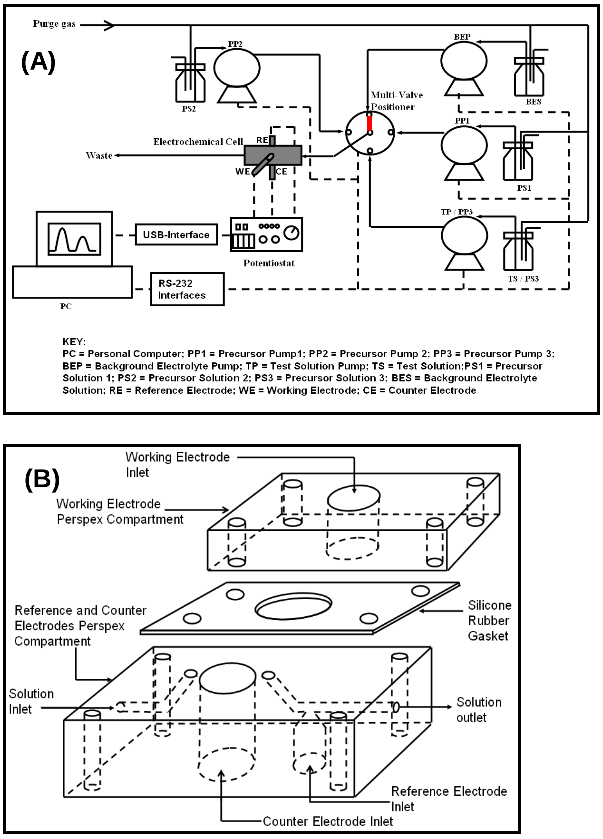

KEY:
PC = Personal Computer; PP1 = Precursor Pump1; PP2 = Precursor Pump 2; PP3 = Precursor Pump 3; BEP = Background Electrolyte Pump; TP = Test Solution Pump; TS = Test Solution;PS1 = Precursor Solution 1; PS2 = Precursor Solution 2; PS3 = Precursor Solution 3; BES = Background Electrolyte Solution; RE = Reference Electrode; WE = Working Electrode; CE = Counter Electrode

Figure 1: (A) Configuration of an automated electrochemical deposition and characterisation apparatus; (B) schematic diagram of components of an electrochemical flow-cell designed and used in this work for electrochemical deposition and characterisation of electrocatalysts.

The flow-cell consisted of two separate Perspex blocks, (i) for insertion of reference and counter electrodes and (ii) for holding the working electrode (or substrate under study). The operational cell was assembled by clamping the two Perspex blocks, sandwiched with the silicone gasket, using four bolts. The reference electrode in the thin-layer cell was a Teflon-based Ag/AgCl/3M KCl (model 6.0727.000, Metrohm, Switzerland) that was placed at the outlet stream of the cell. The transparent Perspex blocks allowed visual monitoring of deposition processes. The working electrode used with the custom-built flow-cell was a glassy carbon (GC) rod (grade V-25, 10 mm long, SPI supplies, USA) embedded in a brass holder that could be secured via fine threading into the Perspex block, exposing a smooth GC surface with diameter = 5 mm, area = 0.20 cm^2 when placed through the Perspex block. The counter electrode was a machined stainless steel rod with threading that allowed it to be directly screwed into the Perspex block exposing a smooth disc of about 0.20 cm^2. A commercial wall-jet cell (model 6.5303.030, Metrohm, Switzerland) equipped with a built-in gold disc (diameter 2 mm) as counter electrode was also used to perform comparative studies on commercial polycrystalline bulk Pt electrode (disc diameter = 2mm, geometric area = 0.03 cm^2, Metrohm, Switzerland).

3. Synthesis of electrocatalysts

The general scheme adopted in this work for formation of monometallic Pt nanostructures on a substrate is illustrated in Figure 2. The extended scheme for stepwise formation of bimetallic Pt-Ru nanostructures/nanofilms is shown in Figure 3.

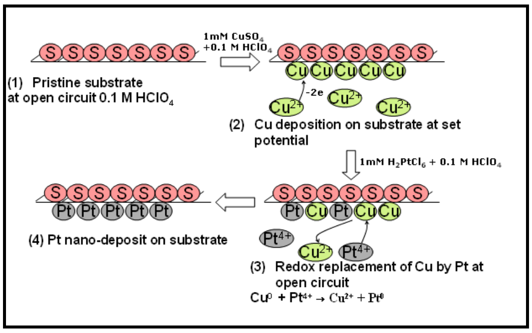

Figure 2: General synthetic scheme adopted in this work for formation of monometallic Pt nanostructures on a substrate. The scheme depicts one deposition cycle.

For simplicity, electrocatalysts/nanostructures involving Pt deposited on glassy carbon will be referred as Pt/GC and those involving Pt and Ru will be abbreviated as Pt-Ru/GC.

Thermodynamic modelling (using FactSage^{TM} version 5.5 9Thermfact and GTT Technologies, Canada, www.factsage.com), was deployed to obtain potential-pH relationships for the Pt-Cu-H_2O and Ru-Cu-H_2O systems to provide some insight and to probe the effect of pH at 25℃ and potentials on the various species of the metals of interest, our main aim being deposition of metallic states via strategies depicted in Figures 1 and 2. For concentrations of 1mM soluble species of Pt, Cu, and Ru, we found that metallic states Pt(s) and Ru(s) co-existed at pH between 0 and 3.5 and potential ranges below +0.4V. Metallic Cu existed at potentials below +0.15 V. From such modelling, deposition experiments were set at pH 1. Moreover, Cu deposition on glassy carbon was studied by cyclic voltammetry and no distinctive UPD potential ranges could be identified. Thus, Cu deposition were run at -0.05 V for various deposition times ranging from 5 s to 150s. Calculations of monolayer-equivalent from the coulombic charges from voltammetric curves (not shown here), led to deductions that 1 monolayer-equivalent of Cu was deposited after 90s. Moreover, literature studies on Cu electrodeposition on GC indicate a fast electrocrystallisation of well-dispersed Cu nanoclusters at such overpotentials where kinetically-controlled deposition of Cu occurs on GC as applied in this work (Zapryanova et al., 2007).

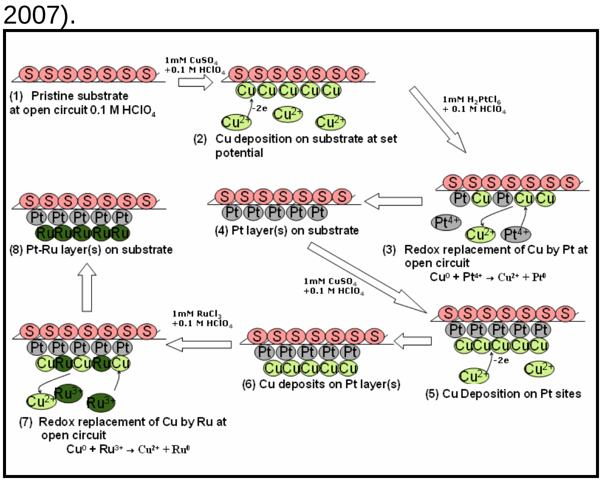

Figure 3: General synthetic scheme adopted in this work for formation of bimetallic Pt-Ru nanostructures. Scheme depicts one deposition cycle.

3.1 Automated synthesis of monometallic systems

Automation of the scheme for synthesis of monometallic Pt supported on GC (Figure 1) was achieved with a LabVIEW program that was developed to perform the necessary sequential steps. The program ran six repeatable main steps depending on the number of cycles desired by alternately directing either the precursor metal solutions (1mM $CuSO_4$ or 1mM H_2PtCl_6 dissolved in 0.1 M $HClO_4$) or the common background electrolyte (BE) solution (0.1 M $HClO_4$) (Three pumps are controlled in this regard) to the electrochemical flow-cell. In depositing Cu templating layer, the first step is the rinsing step where the BE solution is pumped at a desired flow rate to the deposition cell at a set potential for a specific period of time. Secondly, the precursor metal solution ($CuSO_4$) is introduced to the cell at set flow rate and applied potential for a specific duration. Lastly, the precursor pump is stopped to allow deposition in quiescent solution to take place at a set potential for a desired deposition time. The Cu precursor is then rinsed out of the cell with the blank electrolyte, followed by injection of the Pt precursor solution. The injected Pt precursor is then allowed time in the cell, at quiescent conditions for a set duration of time at open circuit, to allow the redox-replacement reaction of the Cu layer(s) by Pt. These steps can be repeated according to the number of cycles desired to increase the amount of Pt layers. During all these steps current and potential that results from the deposition cell are sampled as a function of time to generate online current-potential-time (*I-E-t*) traces. These data can be saved into a spreadsheet format for further analysis that may include coverage per deposition cycle and variation in open circuit potential.

3.2 Automated synthesis of bimetallic systems

The computer program to execute the scheme depicted in Figure 3 to obtain bimetallic films/nanostructures, such as Pt-Ru layers, on a substrate, essentially follows the same sequence of steps as that for monometallic systems described above to deposit the Pt layer. A further sequence involves the use of similar steps to deposit the second element, Ru. The common background electrolyte (0.1M $HClO_4$) is used for rinsing steps and altogether four pumps are utilized.

3.3 Deposition parameters

For Pt/GC, rinsing steps were done at +0.2 V toward deposition of Cu for 20s. The Cu precursor was introduced to the cell at +0.2 V for 20s and Cu deposition was done at controlled potential of -0.05V for 90s as per previous considerations. The cell was then rinsed with the blank at same potential for 20s. The Pt precursor was introduced to the cell at open circuit for 20s and allowed in the cell at quiescent conditions for 180s. This scheme was repeated for up to 8 cycles. For Pt-Ru/GC the same parameters were adopted for deposition of Pt followed by Ru in place of Pt. Again, up to 8 cycles were performed.

3.4 Control experiments

Insights into the growth mechanisms and nature of resulting nanostructures formed via redox-replacement reactions were obtained by performing control experiments involving the use of the same general scheme depicted in Figures 1 and 2 with omission of the Cu deposition steps, whereby such steps were replaced with the blank electrolyte (0.1M $HClO_4$ in replacement of 1mM $CuSO_4$+0.1 M $HClO_4$). All other deposition parameters were maintained constant.

4. Characterisation of electrocatalysts

Electrochemical methods and microscopic investigations (Scanning Electron Microscopy – SEM) were used to probe properties of Pt/GC and Pt-Ru/GC electrocatalysts prepared automatically by schemes discussed above. The inherent advantage of the flow-cell based electrochemical deposition methods deployed in our work was that the as-prepared catalysts could be probed in situ using electrochemical techniques that were part-and-parcel of the deposition setup (see Figure 1). Some representative results are discussed below.

Typical *I-E-t* transients recorded during electrodeposition of Pt-Ru/GC with and without Cu steps are shown in Figure 4. Variations in open circuit potential during Pt and Ru deposition steps clearly show differences in deposition of these noble metals. OCP for Pt varied to about +0.62 V, whereas OCP during Ru deposition step varied to about +0.35V when

Cu steps were involved. The OCP in the control experiments for Pt varied to about +0.65 and for Ru steps to about +0.65 as well.

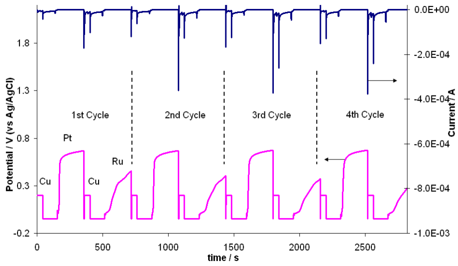

Figure 4 (A): Current-potential-time traces recorded during deposition of Pt-Ru on GC via redox-replacement of Cu.

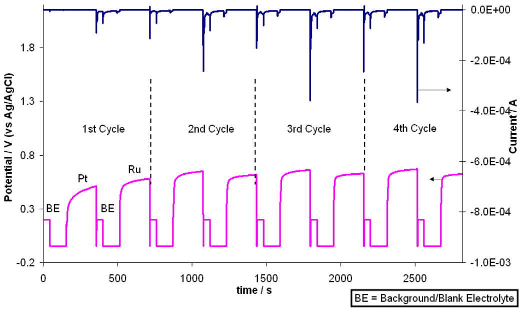

Figure 4 (B): Current-potential-time traces recorded during deposition of Pt-Ru on GC via control experiment (without redox-replacement of Cu).

The OCP during Ru deposition step, via Cu replacement is the range where metallic Ru is expected to be stable, according to thermodynamic models for Ru-Cu-$H_2$0 discussed above. However, this is on thermodynamic grounds and hence, further characterization by independent analytical method to confirm the oxidation state of Ru may be required. The OCP for Ru deposition step in the control experiment is in the range where RuO_2 is the predominant species. Clearly, Cu templating layers produce a marked difference in deposition of Pt-Ru on GC.

Cyclic voltammograms (Figures 5–6) recorded in the background electrolyte (0.1 M $HClO_4$) show typical features of Pt electrochemistry in acidic media (Trasatti and Petrii, 1992, Bard and Faulkner, 2001). As deposition cycles increase, commensurate with increasing Pt loading, the electrochemical active surface area increases as deduced from the hydrogen adsorption peaks as well as Pt surface oxides reduction peaks on the voltammograms (Figures 5-6).

Figure 7 presents typical scanning electron microscopy (SEM) images obtained for the various materials investigated. Good coverage by Pt and Ru particles were obtained on the glassy carbon substrate after 8 deposition cycles via Cu replacement strategy. Energy-dispersive X-ray spectroscopy (EDX), performed during SEM imaging confirmed the presence of Pt and Ru, on the modified GC electrodes, with Pt being the predominant element.

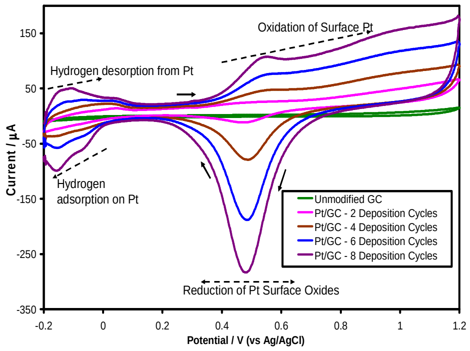

Figure 5: Cyclic voltammograms recorded in 0.1 M $HClO_4$ on glassy carbon immediately after deposition of Pt for various deposition cycles. Scan rate = 50 mV/s. Start potential was -0.2 V.

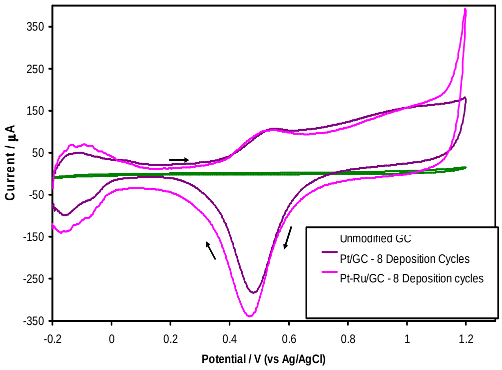

Figure 6: Cyclic voltammograms recorded in 0.1 M $HClO_4$ on glassy carbon before and immediately after deposition of Pt and Pt-Ru for 8 deposition cycles at same conditions. Scan rate = 50 mV/s. Start potential was -0.2 V.

Cyclic voltammetry was employed further to probe activity of the electrocatalysts prepared for electro-oxidation of methanol in acidic media

(Figure 8).The onset potentials on the voltammograms for Pt/GC and Pt-Ru/GC synthesised with the same deposition parameters clearly show positive shift from about +0.5 V for the case of Pt/GC to +0.4 V for the case of Pt-Ru/GC. These observations agree with those made elsewhere in the literature on the promotional effects induced on Pt by Ru, leading to decrease in the overpotential for methanol electro-oxidation (Frelink et al., 1995, Lee et al., 2006), as well as the role of nanostructured electrocatalysts compared to bulk materials (Roth et al., 2008).

So far, our synthetic strategies to synthesise monometallic or bimetallic systems show encouraging promise. Obviously, the conditions used are not necessarily optimal. For example, the Pt-Ru/GC catalyst composition should be varied by employing different deposition conditions and performing more characterisation, to determine mean particle sizes, relative amounts of Pt and Ru, effectively their atomic ratios, and with mechanistic determination of their electrocatalytic properties.

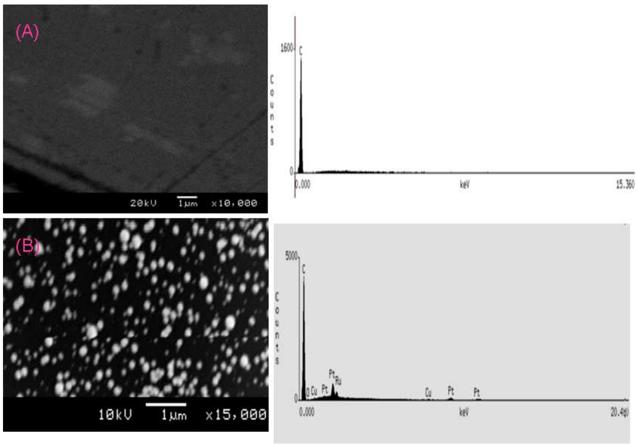

Figure 7: Representative SEM micrographs and corresponding EDX spectra of (A) unmodified GC; (B)Pt-Ru/GC obtained after 8 deposition cycles via redox-replacement of Cu.

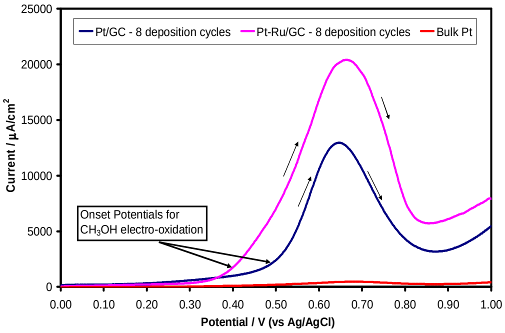

Figure 8: Cyclic voltammograms – forward scans - of bulk polycrystalline Pt electrode, Pt/GC, and Pt-Ru/GC modified electrodes in 0.5 M Methanol + 0.1 M $HClO_4$ solution. Scan rate = 50 mV/s. Current values normalized to geometric areas of the unmodified electrodes.

5. Conclusions

Initial steps towards the demonstration of sequential electrodeposition versatility in synthesis of bimetallic Pt-based nanostructured materials with great potential applications as model fuel cell electrocatalysts are reported. Electrochemical techniques are being implemented in optimization of deposition conditions for a series of other metals, in addition to copper, which may exhibit UPD features on substrates of interest, to synthesise noble-metallic nanostructures via redox-replacement reactions.

Work is also underway in applying surface characterisation techniques such as Scanning Probe microscopy (SPM) and Electrochemical SPM to gain further insights into the influence of topography of substrates on growth mechanisms as implemented in this work, with particular attention to the influence of deposition potentials, electrolytes used, and nature of templating metals. Various carbonaceous as well as metallic substrates, for example polycrystalline Au versus single-crystal Au surfaces, will be explored. Future possible research directions will include mechanistic studies of electrodeposition parameters to synthesise and optimize various Pt-based bimetallic systems of potential use as electrocatalysts.

6. References

Antolini, E. (2007) *Journal of Power Sources,* **170,** 1-12.

Bard, A. and Faulkner, L. R. (2001) *Electrochemical methods: Fundamentals and Applications,* John-Wiley & Sons, Inc, Danvers, USA.

Chu, D. and Gilman, S. (1996) *Journal of the Electrochemical society,* **141,** 1795-1803.

Colletti, L. P., Flowers Jr., B. H. and Stickney, J. L. (1998) *Journal of the Electrochemical Society,* **145,** 1442-1449.

Flowers Jr., B. H., Wade, T. L., Garvey, J. W., Lay, M., Happek, U. and Stickney, J. L. (2002) *Journal of Electroanalytical Chemistry,* **524-525,** 273-285.

Frelink, T., Visscher, W. and van Veen, J. A. R. (1995) *Surface Science,* **335,** 353-360.

Goddard, W., Merinov, B., Van Duin, A., Jacob, T., Blanco, M., Molinero, V., Jang, S. S. and Jang, Y. H. (2006) *Molecular Simulation,* **32,** 251-268.

Gregory, B. W. and Stickney, J. L. (1991) *Journal of Electroanalytical Chemistry,* **300,** 543-561.

Huang, B. M., Colletti, L. P., Gregory, B. W., Anderson, J. L. and Stickney, J. L. (1995) *Journal of the Electrochemical Society,* **142,** 3007-3016.

Innocenti, M., Pezzatini, G., Forni, F. and Foresti, M. L. (2001) *Journal of the Electrochemical Society,* **148,** C357-C362.

Iwasita, T., Hoster, H., John-Anacker, A., Lin, W. F. and Vielstich, W. (1994) *Langmuir,* **16,** 522-529.

Kim, Y.-G., Kim, J. Y., Vairavapandian, D. and Stickney, J. L. (2006) *Journal of Physical Chemistry B,* **110,** 17998-18006.

Koper, M. T. M. (2004) *Surface Science,* **548,** 1-3.

Lee, C.-G., Umeda, M. and Uchida, I. (2006) *Journal of Power Sources,* **160,** 78-89.

Mathe, M. K., Cox, S. M., Flowers Jr., B. H., Vaidyanathan, R., Pham, L., Srisook, N., Happek, U. and Stickney, J. L. (2004) *Journal of Crystal Growth,* **271,** 55-64.

Mathiyarasu, J., Remona, A. M., Mani, A., N., P. K. L. and Yegnaraman, V. (2004) *Journal of Solid State Electrochemistry,* **8,** 968-975.

Papadimitriou, S., A. Tegou, E. Pavlidou, G. kokkinidis and S. Sotiropoulos (2007) *Electrochimica Acta,* **52,** 6254-6260.

Petrii, O. A. (2008) *Journal of Solid State Electrochemistry,* **12,** 609-642.

Pezzatini, G., Caporali, S., Innocenti, M. and Foresti, M. L. (1999) *Journal of Electroanalytical Chemistry,* **475,** 164-170.

Roth, C., Benker, N., Theissmann, R., Nichols, R. J. and Schiffrin, D. J. (2008) *Langmuir,* **24,** 2191 - 2199.

Stickney, J. L., Wade, T. L., Flowers Jr., B. H., Vaidyanathan, R. and Happek, U. (2002) In *Encyclopedia of Electrochemistry*, Vol. 1 (Eds, A.J. Bard and Stratman, M.) Wiley-VCH, Weinheim, pp. 513-560.

Tegou, A., S. Papadimitriou, E. Pavlidou, G. Kokkinidis and S. Sotiropoulos (2007) *Journal of Electroanalytical Chemistry,* **608,** 67-77.

Thambidurai, C., Kim, Y. and Stickney, J. L. (2008) *Electrochimica Acta,* **53,** 6157-6164.

Toda, T., Igarashi, H. and Watanabe, M. (1999) *Journal of Electroanalytical Chemistry,* **460,** 258-262.

Trasatti, S. and Petrii, O. A. (1992) *Journal of Electroanalytical Chemistry,* **327,** 353-376.

Venkatasamy, V., Jayaraju, N., Cox, S. M., Thambidurai, C., Mathe, M. and Stickney, J. L. (2006) *Journal of Electroanalytical Chemistry,* **589,** 195-202.

Vigier, F., Rousseau, S., Coutanceau, C., Leger, J. and Lamy, C. (2006) *Topics in Catalysis,* **40,** 111-121.

Villegas, I. and Napolitano, P. (1999) *Journal of the Electrochemical Society,* **146,** 117-124.

Walters, J. P. (1995) *Analytical Chemistry,* **67,** 34A-35A.

Watanabe, M. (2003) In *Catalysis and Electrocatalysis at Nanoparticle Surfaces*(Eds, A. Wieckowski, E. R. Savinova and Vayenas, C. G.) CRC Press, Boca Raton, pp. Ch. 22.

Yajima, T., H. Uchida and M. Watanabe (2004) *Journal of Physical Chemistry,* **108,** 2654.

Zapryanova, T., Hrussanova, A. and Milchev, A. (2007) *Journal of Electroanalytical Chemistry,* **600,** 311-317.

Zhu, W., Yang, J. Y., Gao, X. H., Bao, S. Q., Fan, X. A., Zhang, T. J. and Cui, K. (2005) *Electrochimica Acta,* **50,** 4041-4047.

7. Endnote:

The authors wish to thank Nico Van Vuuren, mechanical workshop, School of Physical Sciences, University of Pretoria who helped with construction of the flow-cell used in this work. We also wish to thank University of Pretoria to various research facilities and CSIR for parliamentary grant research funding to carry out the work. TSM is thankful to CSIR for a PhD studentship award.